Studies on the physicochemical properties and performance characteristics of the PbO_2 electrode*

F. Bottcher and **H. S. Panesar**
Varta Battery AG Research and Development Centre W-6233 Kelkheim (F R G)

Abstract

At least 10 different parameters have been determined *in situ* as well as *ex situ* and statistically analyzed to study changes in the physicochemical properties of PbO_2 electrodes during the cycle life of traction batteries The specific surface area, water content, microporosity and delta capacity are significant and strongly correlated These variables, together with the high-frequency resistance, monitor the state of the positive active material as a function of the charge/discharge cycle-life Insignificant variations in the resistance/capacitance and the Warburg term during the cycle life suggest that the changes in the properties of positive active material are not associated with the deviation in electrochemical activity A negative correlation between the water content and specific surface area supports the assumption that the water originates from hydrated crystals, hydroxyl groups or protons present in PbO_2 A thermal decomposition mechanism has been proposed that suggests that the number of vacancies in the crystal lattice decreases with cycling and finally the positive active material attains an ideal structure Furthermore, the area of intergrowth of crystals or necks (as proposed in the Kugelhaufen model) seems to exert a significant cause of the changes in the properties of PbO_2 during the cycle life

During charge/discharge cycling, the performance of lead/acid batteries is impaired by the softening and shedding of the positive active material (PAM) [1–3] The latter phenomena are associated with structural changes and are the symptoms of substantial changes that take place in the properties of the active material From studies of positive electrodes with both optical and scanning electron microscopy, Simon and Caulder [4–6] have shown that, after formation, the microstructure is rather dense and uniform After a few cycles, however, there is a change to a continuous network of PbO_2 agglomerates that are surrounded by uniform voids As cycle life proceeds, the PAM converts first to a 'coralloid' form and then becomes increasingly soft and unstable At this stage, shedding occurs and this rapidly increases, in intensity, thus causing a loss of plate capacity The decrease in the stability of the PAM during development of the coralloid structure is accompanied by an increase in electrical resistance It has been claimed [7] that this

*Paper presented at UNESCO Expert Workshop Theory and Practice of the Lead/Acid System, Gaussig, F R G , April 2–5, 1991

0378-7753/91/$3 50

resistance, together with increased grid corrosion, is the reason for the gradual decline in plate capacity

Thermal decomposition data indicate [8] that, in addition to the ageing of the PAM, there is a change in the solid-state properties of the PbO_2 This can be explained by a corresponding change in the degree of disorder in the crystal structure The disorder may be due to Pb-vacancies in which Pb^{4+} is substituted by 4 protons according to the formula

$$Pb^{4+}{}_{1-x/4}O^{2-}{}_{2-x}(OH)^{-}{}_{x}$$

Along with the substitution of Pb^{4+} in the PbO_2 crystal, hydrogen can exist in form of hydroxyl groups, coupled with the reduction of Pb^{4+} to Pb^{2+}, or as interstitial protons with quasi-free electrons [9–14]

The exponential contraction of the half-width-value of the X-ray diffraction signals of β-PbO_2 indicates that the changes in the material properties are the result of PbO_2 attaining an ideal structure This means that the number of the defects in the crystal structure decreases with increasing cycle number [15, 16] These observations have given rise to the 'hydrogen-loss' model proposed by Caulder *et al* [6] which suggests that an inactive form of PbO_2 may be formed in increasing amounts during cycling The electrochemical activity has been linked with the presence of hydrogen in the crystal lattice In spite of a large number of investigations, a relationship between the content of hydrogen in the crystal lattice of PbO_2 and the capacity loss has not been established [17–23] The results of the various studies are more or less ambiguous or contradictory

Recently, a new model to interpret the structure of the PbO_2 electrode has been proposed [24, 25] in which the PAM is considered to be an aggregate of spheres and the properties of the electrode are governed by the neck zones at the points of contact of these spheres (the Kugelhaufen electrode) Nevertheless, there is no unequivocal model for describing the transformations of the PAM during the progress of charge/discharge cycles

The non-linear coupling of the different material properties complicates the interpretation of the experimental results Therefore, univariate or bivariate methods are not suitable approaches for investigating the electrochemistry of the PbO_2 electrode in porous systems A multivariate method, that is mainly based on Principal Component Analysis (PCA) together with the state space concept, has therefore been applied here to study this phenomena

A formal approach to a multivariate method is based on the concept that the ageing of the active material can be expressed by the change in a p-dimensional state function The state of a complex system is given by p measurable variables, whereby each variable describes the behaviour of one material property

A useful geometric representation of the state of the active material could be conceived by setting up a Euclidian space of p dimensions, one for each variable In this case, the state of a specified sample can be represented by a point in the p-dimensional space The measurement of each

of the p variables on n different samples therefore gives an accumulation of n points in the p-dimensional space

The change in the state of a sample produced by the progress of charge/discharge cycles is now given by a curve in the p-dimensional space In a formal description, the set of p observations on n independent samples can be summarized in the $p \times n$ dimensional observation matrix R

The change in the state of the samples as a result of the cycling procedure maps the initial matrix R on to the new matrix R' Using a mathematical formulation, the mapping is generated by the non-linear and time-dependent matrix T, i e ,

$$R'(t) = T(t)\ R\ (t = 0) \tag{1}$$

If only the state of the completely charged mass is monitored and it is assumed that every cycle consists only of a simple discharge followed by a charge process, then, as a useful simplification, a non-time-dependent matrix T' is obtained In this representation, one cycle transforms the mass properties R_0 to the properties R_1, the next to R_2 and so on, i e ,

$$R_i = T^n R_0 = TTTT \quad R_0 \tag{2}$$

If special cycle conditions only affect the short-time-memory of the PAM, as represented by the transformation

$$R_{rev} = T_{rev} R_0 \tag{3}$$

there exists a cycle condition T_{rev} , which compensates the variation of the material properties

$$R_0 = T_{rev}\ R_{rev}$$

The ageing of the active material as a result of a progress of charge/discharge cycles is given, therefore, by the irreversible part of R, namely

$$R_{irr} = R - R_{rev} \tag{4}$$

Although, to date, it is not known how T can be expressed, the investigation of the point distribution in the state space gives considerable insight into the transformation of the PAM during the cycle life

In a practical approach, the different states of the samples at the beginning and at the end of the cycle test can be visualized as two point clusters in a plane that is given as a section through the region of the state space that covers the highest point density This section is given by the first two principal components of the PCA

The basic idea of the PCA is to find a linear transformation of the starting coordinate system in such a way that each of the axes of the new coordinate system is a linear function that gives a closest fit to the points in the space [26] As a limitation, the linear function has to be orthogonal The first axis, or principal component (PC1), passes through the centre of gravity of the points in the state space The second principal component (PC2) passes through the centre of gravity orthogonal to PC1 and so on

The new coordinates are the eigenvalues of a matrix R which is built up by the complete set of observations Therefore it follows that

- the largest eigenvalues contain the most useful information relating to the specific problem,
- the remaining eigenvalues mainly comprise noise,
- by plotting the largest eigenvalues against each other, a plot of the distribution of the points in space is obtained [27],
- the variables that have significant contributions to one eigenvector are correlated The components of the eigenvectors are calculated in a standardized form This means that each component is present in the range -1 and $+1$ As a rule-of-thumb, absolute component values higher than 0 5 indicate significant contributions

On account of the latter feature, it is possible to achieve a separation between the errors and the significant data of experimental results and to elicit information about the main correlation between the variables The calculation of the PCA was carried out using a minicomputer The software, which has been applied, was based on modules from the IMSL-Statistic FORTRAN Library

As mentioned above, in order to construct the state space, it is necessary to define a set of variables that describe the properties of the PAM As a first approach, the electrode should be divided into a set of 4 sub-systems that determine simultaneously the performance characteristics of the whole system, namely

1 Macro/microstructure of the PAM
2 Solid-state properties of the PAM
3 The interface electrolyte/PbO_2
4 The interface PbO_2/grid

Each sub-system is characterized by a set of variables as follows

Characterization of sub-system 1

The macro/microstructure is realized with the variables surface area, total porosity, pore size distribution, micro-porosity (pore radius < 1000 Å), electric resistance (determined as the high-frequency resistance of the impedance spectrum)

Characterization of sub-system 2

The solid-state properties are realized with the variables water-content, high-frequency resistance The PAM samples were dried at 60 °C for 24 h under vacuum and then stored in a desiccator at room temperature The water content was determined in the temperature range 240 to 450 °C using the Karl Fischer titration method

Characterization of sub-system 3

The electrolyte/PbO_2 interface is characterized by the exchange-current density and the double-layer capacity The determination of these values was achieved indirectly by impedance spectroscopy Measurements were conducted between 60 kHz and 0 02 Hz with a reference voltage of 1 175 V This is 20 mV above the open-circuit value A typical result is given in Fig 1

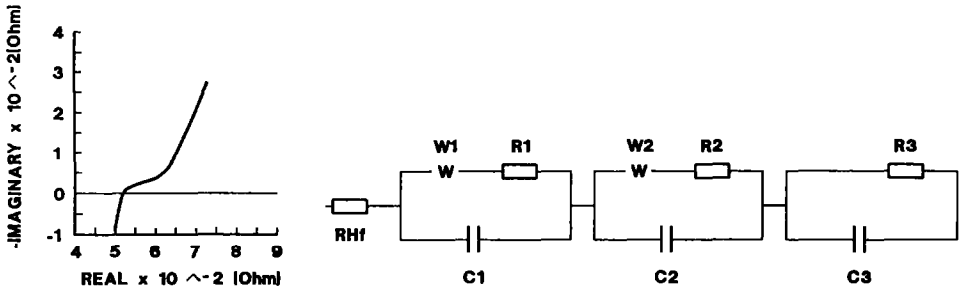

Fig 1 Impedance data for electrolyte/PbO_2, interface

Fig 2 Equivalent circuit for processes occurring at PbO_2 electrode

Assuming that the impedance can be expressed as a series/parallel combination of resistors, capacitors and Warburg terms, the model shown in Fig 2 was used for the interpretation of the measurements The model consists mainly of the high-frequency resistance R_{HF} and three *RC*-terms A Warburg term is included in the first 2 *RC*-terms It is assumed that the first term includes the kinetics of the proton exchange in the macropores while the second term represents the water decomposition in the micropores The third term consists of a high resistance ($>1\ \Omega$) and a capacitance (150 to 250 F) The magnitude of the capacitance can be compared with the delta capacity [10, 25, 28–30] It is also assumed that the kinetics and, therefore, the electrochemical activity are related to the variables *W*1 to *C*2

Characterization of sub-system 4

The grid/PbO_2 interface indirectly results from the degree of the grid corrosion This is determined by the change in the electrical resistance of the grid

In order to reduce the number of state variables and to come to a comprehensible relationship between ageing and electrochemistry, an attempt was made to eliminate variables Variations in the latter are mainly influenced by short-time memory effects For this reason, two different groups of commercial traction batteries were investigated the first group comprised batteries that had undergone only 3 months of laboratory testing, the second group were batteries that had completed ~50 months of service The older batteries were under a random stress condition in an industrial environment By contrast, the 3-month-old batteries had experienced only 50 cycles under standard conditions

Before measurement of the state variable, all batteries were subjected to a standard cycling procedure in order to ensure a comparable start condition From all the different batteries, a total of 42 electrode samples were placed in a special test set-up (Fig 3) so as to determine the capacity and the impedance diagram After removing, washing and drying the test electrodes, the other variables were determined

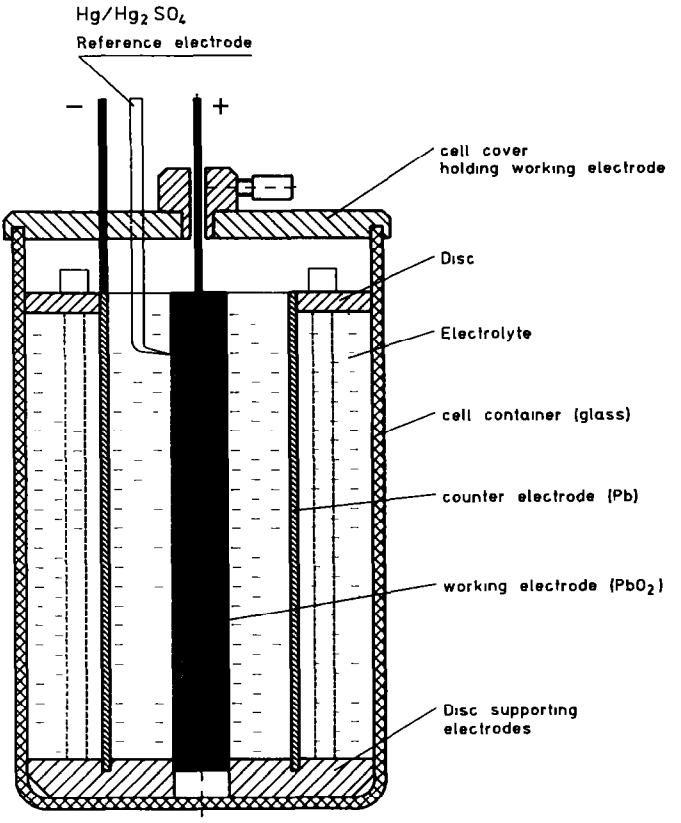

Fig 3 Schematic of test cell

Independent measurements of 13 variables on 42 different samples give a cluster of 42 points in the 13-dimensional state space Corresponding to the two different cycle lives of the samples, these clusters of points should be divided into two groups To prove this hypothesis the principal component analysis (PCA) is applied

In a first attempt, 10 variables (namely, grid resistance, water content, specific surface area, porosity, microporosity, high-frequency resistance, $R1$, $C1$, $R2$ and $C2$) were taken into the PCA The results are shown in Table 1 The first 4 eigenvalues represent 80% of the total variance

The first vector comprises mainly the water content (C_{H_2O}), specific surface area (BET), microporosity, high-frequency resistance (R_{HF}) and $C1$ This represents a significant correlation between these variables The second eigenvalue shows a significant correlation between the specific surface area and the variables R_{HF}, $R1$ and $C1$ given by the impedance spectroscopy. The third eigenvalue represents a significant correlation between porosity and grid corrosion The other eigenvalues represent indifferent weak correlations between all variables and mainly comprise noise

TABLE 1

Eigenvectors and eigenvalues of the principal component analysis based on the variables C_{H_2O}, R_S, *BET*, porosity, microporosity, R_{HF}, *C*2, *R*2, *C*3, *R*3

Vectors	1	2	3	4	5	6	7	8	9	10
EVEC[a]	2 754	2 204	1 804	1 604	0 629	0 493	0 423	0 367	0 172	0 000
PCT[b]	0 264	0 474	0 647	0 801	0 861	0 908	0 948	0 984	1 000	1 000
A[c]										
R_S	0 4198	0 2059	0 7108	0 3177	0 0732	−0 2710	0 1851	0 1269	0 2144	0 0000
C_{H_2O}	−0 6861	0 4018	0 2650	−0 1126	−0 0132	0 4088	−0 0287	0 3303	0 0880	0 0000
BET	0 7149	−0 5337	−0 2195	−0 0421	−0 0065	0 3189	−0 0497	−0 0783	0 2091	0 0000
Porosity	0 1116	−0 1075	0 8364	0 0756	0 3726	0 1744	−0 2344	−0 1882	−0 1052	0 0000
Microporosity	0 6899	−0 5579	0 0936	−0 0646	0 0585	0 0504	0 1503	0 3631	−0 1985	0 0000
R_{HF}	0 5922	0 6765	−0 1502	−0 3811	0 1018	−0 0205	−0 1071	0 0387	−0 0067	−0 0003
*C*2	0 2601	0 5697	−0 1610	0 5834	0 0628	0 2779	0 3611	−0 1511	−0 0846	0 0000
*R*2	0 5922	0 6765	−0 1502	−0 3811	0 1018	−0 0205	−0 1071	0 0387	−0 0067	0 0003
*C*3	0 3634	0 1972	0 0229	0 7372	−0 3861	0 0098	−0 3528	0 0959	−0 0459	0 0000
*R*3	−0 2087	−0 0713	−0 5881	0 5117	0 5398	−0 0923	−0 1350	0 1518	0 0498	0 0000

[a]EVEC eigenvalues

[b]PCT cumulative % of total variance explained by each eigenvalue

[c]A standardized eigenvectors

If the first principal component is plotted against the second, a weak separation of the two point groups is observed (Fig 4) Both groups are associated with the different age of the samples

A detailed analysis of the second and third principal components shows that the corresponding variables are not or indefinitely dependent on the age of the samples Thus, in the view of the aim of this study, the associated variables in the next step of the analysis are neglected

The variables that yield the most significant contributions to the first eigenvector are taken into a new PCA Other results have shown that the variables $W1$ and $C3$ of the impedance spectroscopy should also be considered The result of this PCA is presented in Table 2 With the exception of the high-frequency resistance, all variables make significant contributions to the first eigenvalue This means that these variables are strictly inter-dependent The second eigenvalue mainly consists of the high-frequency resistance with significant contributions from the microporosity and $C3$ The other eigenvalues comprise noise or show an internal correlation of $W1$ and $C3$

The plots of the first principal components show two separated clusters of points that represent the two groups of battery samples with different cycle numbers (Fig 5) This shows that the concept of state space combined with PCA is an efficient approach for analyzing the ageing of the positive active material in lead/acid batteries

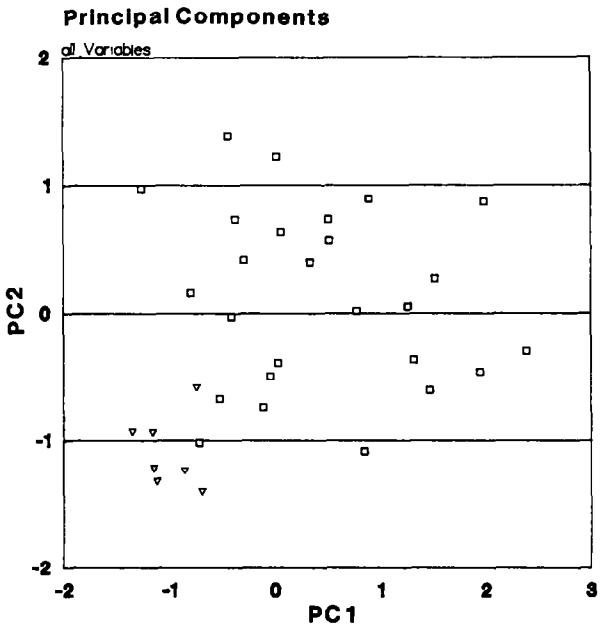

Fig 4 Principal component analysis of (□) old batteries, (▽) new batteries

TABLE 2

Eigenvectors and eigenvalues of the principal component analysis based on the variables C_{H_2O}, *BET*, microporosity, R_{HF}, *W*2, *C*2

Vectors	1	2	3	4	5	6
EVEC[a]	2 910	1 523	0 709	0 612	0 361	0 230
PCT[b]	0 459	0 699	0 810	0 907	0 964	1 000
A[c]						
C_{H_2O}	−0 8227	0 1614	0 0011	0 3151	0 4345	0 0953
BET	0 8519	−0 3513	0 0804	0 0769	0 2818	−0 2429
Microporosity	0 7028	−0 5284	−0 1797	0 3155	−0 0288	0 3070
R_{HF}	0 4007	0 7236	−0 0484	0 5266	−0 1581	−0 1063
*W*2	0 6099	0 4660	0 5838	−0 1553	0 1032	0 1877
*C*2	0 5244	0 5400	−0 5543	−0 2984	0 1812	0 0662

[a]EVEC eigenvalues

[b]PCT cumulative % of total variance explained by each eigenvalue

[c]A standardized eigenvectors

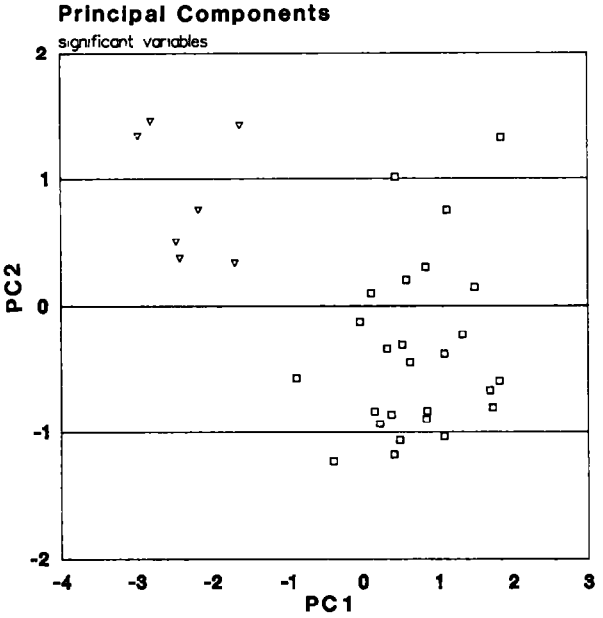

Fig 5 Principal component analysis of (□) old batteries, (▽) new batteries

Conclusions

The specific surface area, the water content, the microporosity and the delta capacity are significant and strongly correlated These variables, together with the high-frequency resistance R_{HF}, monitor the state of the positive active material as a function of the charge/discharge cycle life

The insignificant variations in the resistance/capacitance and the Warburg term during the cycle life suggest that the changes in the properties of the positive active material are not associated with the deviation in electrochemical activity

A negative correlation between the water content and specific surface area supports the assumption that the water originates from hydrated crystals, hydroxyl groups or protons present in PbO_2 Therefore, the following thermal decomposition mechanism seems very likely

$$PbO_2H_x \; nH_2O \longleftrightarrow Pb_{1-x/2}{}^{4+}Pb_{x/2}{}^{2+}O_2{}^{2-}H_x{}^{+} \; nH_2O \longleftrightarrow$$

$$Pb_{1-x/2}{}^{4+}Pb_{x/2}{}^{2+}O_{2-x/2}{}^{2-} \; (n+x/2)H_2O \xrightarrow{>240\,^{\circ}C} PbO_x + (n+x/2)H_2O$$

The average water content decreases from $0\,67 \pm 0\,03\%$ in laboratory test batteries (3-month-old) to $0\,46 + 0\,01\%$ in the 50-month-old samples Considering the mechanism suggested above, these results show that the number of vacancies in the crystal lattice decreases with cycling The lack of correlation between the high-frequency resistance and the water content indicates that

the decrease in the number of vacancies is not linked to a significant increase in the resistance of the positive active material The absence of a correlation between the degree of corrosion and the high-frequency resistance shows that increase in the latter cannot be explained by a passive layer in the corrosion zone at the grid/active-material interface or by changes in the solid-state properties of the positive active material Therefore, the increase in the high-frequency resistance appears to be due to the resistance resulting from the surface area caused by the intergrowth of PbO_2 crystals During ageing, the positive active material attains more and more an ideal structure This suggests that both the number of vacancies and the disorder in PbO_2 crystals gradually decrease

From the above results, it can be concluded that changes in the properties of the PbO_2 electrode during cycle life in terms of changes in the area of the intergrowth of crystals or necks (i e , the Kugelhaufen model) are of significant importance in the electrochemistry of PbO_2.

References

1 K Harris, R J Hill and D A J Rand, *J Electrochem Soc , 131* (1984) 474
2 E Voss and G Huster, *Chem -Ing -Techn , 38* (1966) 623–626
3 E Voss and G Huster, Performance forecast of selected static energy conversion devices, *29th Advisory Group for Aerospace Research and Development (AGARD) Meet , Liège, 1967*, pp 57–72
4 A C Simon and S M Caulder, *J Electrochem Soc , 118* (1971) 659
5 S M Caulder, J S Murday and A C Simon, *J Electrochem Soc , 120* (1973) 1515
6 A C Simon, S M Caulder and J T Stemmle, *J Electrochem Soc , 122* (1975) 461
7 S M Caulder and A C Simon, *J Electrochem Soc , 121* (1974) 1546
8 N J Maskalick, *J Electrochem Soc , 122* (1975) 20
9 R J Hill and I C Madsen, *J Electrochem Soc , 131* (1984) 1486
10 H Rickert, *Z Phys Chem Neue Folge, 95* (1975) 47
11 J P Pohl and H Rickert, *Z Phys Chem Neue Folge, 95* (1975) 59
12 J P Pohl and H Rickert, *J Power Sources, 6* (1976) 59
13 J R Gavarri, P Garnier, P Boher, A J Dianoux, G Chedeville and B Jacq, *J Solid State Chem , 75* (1988) 251
14 R Varma, J Eckert, V A Maroni, J A Goldstone, C Giodano, R Cehelnik, R Kumar, S Siegel and B Tani, in K R Bullock and D Pavlov (eds), *Proc Symp Advances in Lead-Acid Batteries*, Proc Vol 84–14, The Electrochem Soc , Inc , Pennington, NJ, U S A , 1984, p 45
15 M Yamaura, M Kohno, Y Ohtani, M Yamane and N Nakashima, *ILZRO Project LE-197, Rep for Period Mar 1972–Mar 1973*, International Lead Zinc Research Organization, Inc , Research Triangle Park, NC, U S A , 1973
16 T G Chang, *J Electrochem Soc , 131* (1984) 1755
17 J Yamashita, H Yutu and Y Matsumaru, *YUASA-JIHO (Technical Review), 67* (1989) 4 (published by YUASA Battery Co Ltd , Tatasuki, Osaka, Japan)
18 J Yamashita and Y Matsumaru, *J Appl Electrochem , 18* (1988) 595
19 A Santoro, P D'Antonio and S M Caulder, *J Electrochem Soc , 130* (1983) 1451
20 J D Jorgensen, R Varma, F J Rotella, G Cook and N P Yao, *J Electrochem Soc , 129* (1982) 1678
21 P T Moseley, J L Hutchinson, C J Wright, M A M Bourke, R I Hill and V S Rainey, *J Electrochem Soc , 130* (1983) 829
22 R J Hill and A M Jessel, *J Electrochem Soc , 134* (1987) 1326

23 D Pavlov, E Bashtavelova, V Manev and A Nasalevska, *J Power Sources*, *19* (1987) 15
24 U Hullmeine, A Winsel and E Voss, *J Power Sources*, *25* (1989) 27
25 E Voss, *J Power Sources*, *7* (1982) 343
26 S Wold, K Esbensen and P Geladi, *Chemometrics Intelligent Lab Sys*, *2* (1987) 37
27 R A Cole and K Phelps, *J Sci Food Agric*, *30* (1979) 669
28 W Fischer and H Rickert, *Ber Bunsenges Phys Chem*, *77* (1973) 975
29 J P Pohl and H Rickert, *Z Phys Chem*, *112* (1978) 117
30 J Bohmann, U Hullmeine, W Kappus, E Voss and A Winsel, *ILZRO PROJECT LE-277, Rep for Period July 1-Dec 31 1981*, International Lead Zinc Research Organization, Inc, Research Triangle Park, NC, U S A, 1981